

Improved prediction scheme for ion heat turbulent transport

Cite as: Phys. Plasmas **29**, 102505 (2022); <https://doi.org/10.1063/5.0103447>

Submitted: 15 June 2022 • Accepted: 11 September 2022 • Published Online: 12 October 2022

 M. Nunami,  S. Toda,  M. Nakata, et al.

COLLECTIONS

 This paper was selected as an Editor's Pick



View Online



Export Citation



CrossMark

ARTICLES YOU MAY BE INTERESTED IN

[A numerical approach to the calculation of the Alfvén continuum in the presence of magnetic islands](#)

Phys. Plasmas **29**, 092102 (2022); <https://doi.org/10.1063/5.0102239>

[Announcement: The 2021 James Clerk Maxwell prize for plasma physics](#)

Phys. Plasmas **29**, 070201 (2022); <https://doi.org/10.1063/5.0106539>

[Linear stability analysis via simulated annealing and accelerated relaxation](#)

Phys. Plasmas **29**, 102504 (2022); <https://doi.org/10.1063/5.0101095>

Physics of Plasmas

Special Topic: Plasma Physics
of the Sun in Honor of Eugene Parker

Submit Today!

Improved prediction scheme for ion heat turbulent transport

Cite as: Phys. Plasmas **29**, 102505 (2022); doi: [10.1063/5.0103447](https://doi.org/10.1063/5.0103447)

Submitted: 15 June 2022 · Accepted: 11 September 2022 ·

Published Online: 12 October 2022



View Online



Export Citation



CrossMark

M. Nunami,^{1,2,a)}  S. Toda,^{1,3}  M. Nakata,^{1,3,4}  and H. Sugama^{1,5} 

AFFILIATIONS

¹National Institute for Fusion Science/National Institutes of Natural Sciences, Toki, Gifu 509-5292, Japan

²Graduate School of Science, Nagoya University, Nagoya, Aichi 464-8601, Japan

³The Graduate University for Advanced Studies, SOKENDAI, Toki, Gifu 509-5292, Japan

⁴PRESTO, Japan Science and Technology Agency, Kawaguchi, Saitama 332-0012, Japan

⁵Department of Advanced Energy, University of Tokyo, Kashiwa, Chiba 277-8561, Japan

^{a)} Author to whom correspondence should be addressed: nunami.masanori@nifs.ac.jp

ABSTRACT

A novel scheme to predict the turbulent transport of ion heat of magnetic confined plasmas is developed by combining mathematical optimization techniques employed in data analysis approaches and first-principle gyrokinetic simulations. Gyrokinetic simulation, as a first-principle approach, is a reliable way to predict turbulent transport. However, in terms of the flux-matching [Candy *et al.*, Phys. Plasmas **16**, 060704 (2009)], quantitative transport estimates by gyrokinetic simulations incur extremely heavy computational costs. In order to reduce the costs of quantitative transport prediction based on the gyrokinetic simulations, we develop a scheme with the aid of a reduced transport model. In the scheme, optimization techniques are applied to find relevant input parameters for nonlinear gyrokinetic simulations, which should be performed to obtain relevant transport fluxes and to optimize the reduced transport model for a target plasma. The developed scheme can reduce the numbers of the gyrokinetic simulations to perform the quantitative estimate of the turbulent transport levels and plasma profiles. Utilizing the scheme, the predictions for the turbulent transport can be realized by performing the first-principle simulations once for each radial position.

Published under an exclusive license by AIP Publishing. <https://doi.org/10.1063/5.0103447>

I. INTRODUCTION

In magnetic confined fusion plasma research, first-principle simulation based on gyrokinetic model¹ is a powerful and reliable means to predict the turbulent transport or profiles of plasma temperatures and densities. Indeed, it has been possible to validate local gyrokinetic simulations against experimental observations of transport fluxes within experimental errors.^{2–5} For the predictions, there are two main approaches. One is to perform many first-principle gyrokinetic simulations, which is the so-called flux-matching technique.^{6,7} The other is to employ the quasi-linear transport model^{8–10} or the reduced transport model¹¹ with reduced calculation costs.

In the former approach, based on the flux-matching technique, by performing gyrokinetic simulations while changing the input parameters for the plasma profiles, e.g., radial gradients of the temperatures and densities, we can find the transport fluxes that agree with the experimental observations quantitatively. Furthermore, the flux-matching approaches are also significant to quantitatively estimate the discrepancies against the experiment in order to clarify the validity of

the physical model used in the simulation. However, to obtain such matched transport fluxes, numerous gyrokinetic runs should be demanded. Even in the simplest case of the ion temperature gradient turbulence with a single-ion-species plasma, the conventional flux-matching technique demands several nonlinear runs for each radial position, to find out the matched transport flux. Therefore, in particular, for cases of multi-ion-species plasmas including kinetic electrons, we must perform a huge number of the simulations in a multi-dimensional space of the temperature and density gradients which exponentially expands with increasing numbers of species. For example, in the case of three ion-species plasma⁴ in the large helical device (LHD),¹² the flux-matching technique has been performed while changing the temperature gradients and density gradients of electrons and ions. In the case, we perform over 50 nonlinear gyrokinetic runs at certain radial position, to obtain the heat transport flux matched region of the ion and electron temperature gradients, where the heat transport fluxes of each ion species can match the experimental observations. Of course, in more realistic cases with many ion species

plasmas, we have to perform the gyrokinetic runs not only for changing the gradients of temperature and density but also the ratios of densities and temperatures between each species, to find the matched parameter region for multi-transport fluxes of heat and particles. Therefore, in such realistic cases, extremely numerous runs are needed for the flux-matching technique.

In the latter approach to predict the plasma transport, we employ reduced transport models, which are constructed by the results of many nonlinear gyrokinetic simulations and the linear or quasi-linear analysis. In the approach, the reduced transport model enables us to obtain the turbulent transport fluxes without additional nonlinear gyrokinetic simulations. However, since such reduced transport models are constructed by limited numbers of parameters of the plasma profiles for the various cases of the plasmas, the models essentially include certain prediction errors. Especially in marginal instability regions of the temperature or density gradients, the prediction errors will be crucial, because a sensitive dependence of the turbulent transport on radial gradients of the temperatures or densities, namely, profile stiffness, may enhance the error impacts.

In this work, we propose a novel scheme to predict the turbulent transport, focusing on ion heat transport as a simple example. In the developed scheme, we combine first-principle simulations using the local flux-tube gyrokinetic code GKV,¹³ the reduced transport model, and mathematical optimization techniques. Using the developed scheme, we can reduce the numbers of first-principle gyrokinetic simulation runs as much as possible, securing the accuracy of estimates of turbulent transport levels. We apply the scheme to estimate ion heat transport, and we achieve reliable and efficient predictions for the turbulent ion heat transport and the ion temperature profiles.

This paper is organized as follows. In Sec. II, the transport prediction scheme developed in this paper is introduced. In Sec. III, the developed scheme is applied to the ion heat transport analysis and a prediction of the radial profile of the ion temperature for LHD plasma. Finally, we summarize the work in Sec. IV.

II. A TRANSPORT PREDICTION SCHEME

A. Reduced transport model

For simplicity, we consider the ion heat transport caused by the turbulences driven by the ion temperature gradient (ITG) instability under the adiabatic electron response assumption. In order to reduce numbers of the first-principle gyrokinetic simulations as much as possible, it is significant to find relevant input parameter of the ion temperature gradient for the gyrokinetic simulations, to realize the resultant transport fluxes, which is close to the experimental results. In the developed scheme, we employ the reduced transport model for ion heat diffusivity based on the previous our work¹⁴ for the LHD plasma to find the relevant input parameters of the first-principle simulation. The reduced transport model consists of the turbulent contribution \mathcal{L} , which enhances the transport levels and the zonal-flow contribution τ_{ZF} , which reduces the transport levels represented as the following form:

$$\frac{\chi_i^{\text{model}}}{\chi_i^{\text{GB}}} = \frac{A_1 \mathcal{L}^{\alpha_0}}{A_2 + \tau_{ZF} / \mathcal{L}^{1/2}}. \quad (1)$$

Here, the turbulent contribution \mathcal{L} is a radial function that is given by

TABLE I. Coefficients in the functions $R/L_{Ti}^{\text{cr}}(\rho) = \sum_j B_j^{\text{cr}} \rho^j$, $a(\rho) = \sum_j B_j^a \rho^j$, and $\tau_{ZF}(\rho) = \sum_{j=0} B_j^{\tau} \rho^j$ for the LHD plasma focused in this paper.

	$j=0$	1	2	3	4
B_j^{cr}	4.0929	-3.7681	19.712	11.087	-14.272
B_j^a	0.386 61	-0.070 919	0.2571	0.959 49	-0.929 78
B_j^{τ}	0.985 65	-0.659 43	2.4471	3.2337	-2.8382

$$\mathcal{L}(\rho) \equiv a(\rho) \left[\frac{R}{L_{Ti}(\rho)} - \beta_0 \frac{R}{L_{Ti}^{\text{cr}}(\rho)} \right], \quad (2)$$

with the ion temperature gradient length $L_{Ti}(\rho)$ defined by $L_{Ti}^{-1}(\rho) \equiv -(1/r_l) d(\ln T_i) / d\rho$ with the normalized radial coordinate $\rho = \sqrt{\Psi / \Psi_l}$, where Ψ is the toroidal magnetic flux, and Ψ_l and r_l are the magnetic flux and minor radius at the last closed surface, respectively. The critical temperature gradient of the linear ITG instability is approximated as a function of $R/L_{Ti}^{\text{cr}}(\rho) = \sum_{j=0} B_j^{\text{cr}} \rho^j$ from the linear instability analysis for the target plasma and the coefficients are estimated up to fourth order of ρ in the previous work,¹⁴ and $\tau_{ZF}(\rho) \equiv \int_0^{\tau_i} dt \langle \phi_{kx, ky=0}(t) \rangle / \langle \phi_{kx, ky=0}(0) \rangle (\rho)$ is the zonal-flow decay time that is determined by the linear zonal-flow response analyses for the electrostatic potential ϕ , where the decay time is also approximated by similar form $\tau_{ZF}(\rho) = \sum_{j=0} B_j^{\tau} \rho^j$. $a(\rho) = \sum_{j=0} B_j^a \rho^j$ is the radial function obtained in our initial model construction via the linear instability analysis.¹⁴ The coefficients in the functions $L_{Ti}^{\text{cr}}(\rho)$, $a(\rho)$, and $\tau_{ZF}(\rho)$ for the LHD plasma, which will be discussed in Sec. II B, are shown in Table I. On the other hand, $A_1 = 1.8 \times 10^1$, $A_2 = 5.2 \times 10^{-1}$, $\alpha_0 = 0.38$, and $\beta_0 = 1.0$ are given as constants that can be applicable to wide range of ITG cases of LHD plasmas, and they are treated as common parameters for whole radial positions in the model. Therefore, these common parameters are independent of the radial positions. Finally, $\chi_i^{\text{GB}} = \rho_{Ti}^2 v_{Ti} / R$ is the gyro-Bohm diffusivity, ρ_{Ti} is the ion thermal gyro radius, v_{Ti} is the ion thermal speed, and R is the major radius.

B. Scheme for transport prediction

As shown in Fig. 1, the scheme developed here basically consists of three steps as follows:

- (i) Guess the initial inputs for gyrokinetic simulations,
- (ii) Run the trial gyrokinetic simulations,
- (iii) Optimize and apply the transport model for transport prediction.

Due to the flow of the scheme above, at the first step (i), using the reduced transport model in Eq. (1) and the mathematical optimization technique in the machine learning numerical library,¹⁵ we search the relevant initial guess of the input parameter of the ion temperature gradient, which realizes the ion heat transport flux $Q_i = -n_i \chi_i \nabla T_i$ that agrees with experimental observations in the target plasma. Here, we employ the most basic technique of the optimizations, gradient descent optimizer¹⁶ or Adam optimizer¹⁷ as an example. Of course, we are free to choose any optimization techniques because it is only essential to find the point in the input parameter space which is the

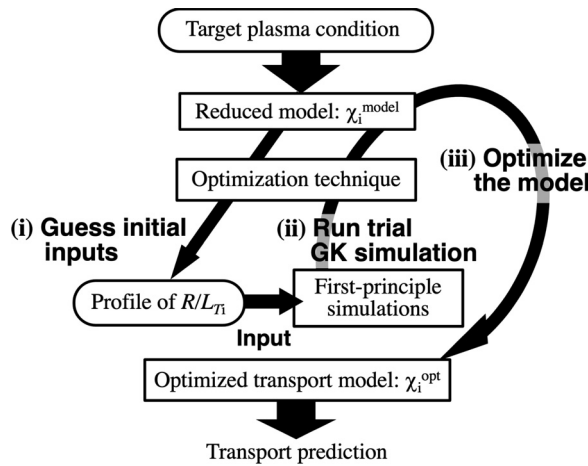


FIG. 1. A schematic flow diagram of the developed scheme combining first-principle gyrokinetic simulations, the reduced transport model, and the optimization technique. The scheme consists of three steps.

closest to the experimental observations. Then, we obtain guessed temperature gradients $R/L_{T_i}^{(guess)}$ at each radial position.

At the second step (ii), using the guessed parameters for the ion temperature gradients, “trial” runs of the first-principle gyrokinetic simulations are performed once for each radial position by the GKV code. Then, the turbulent ion heat fluxes or the ion heat diffusivity χ_i^{trial} at the guessed temperature gradients $R/L_{T_i}^{(guess)}$ at each radial position can be obtained.

At the final step (iii), using the results of the trial gyrokinetic runs at several radial positions, the optimization technique is applied to optimize the reduced transport model by tuning the common parameters in the initial model among whole radial positions. Here, as an example of the optimization technique, we employ the Levenberg–Marquardt method,^{18,19} which is one of the nonlinear

function optimization techniques. Although all common parameters of the reduced model in Eq. (1) and (2) can be tuned for the optimization, here we focus on two common parameters α_0 and β_0 in the model, because they have a strong influence on the transport coefficients in the marginal temperature gradient region. In the optimization, we try to minimize the objective function defined as

$$\sigma(\alpha, \beta) \equiv \left[\frac{1}{N_{\text{trial}}} \sum_j \left(\frac{\chi_{i,j}^{\text{model}}}{\chi_{i,j}^{\text{trial}}} \bigg|_{[R/L_{T_i}^{(\text{guess})}]_j} - 1 \right)^2 \right]^{1/2}, \quad (3)$$

in the parameter space of $\{\alpha, \beta\}$ instead of $\{\alpha_0, \beta_0\}$. Here, N_{trial} is the total number of the trial gyrokinetic simulations. After the optimization process, we can obtain the optimized values $\alpha_0 \rightarrow \alpha$, and $\beta_0 \rightarrow \beta$ to cover all trial gyrokinetic results at different radial positions. In this way, by a few run of the nonlinear gyrokinetic simulation at each radial position, we can obtain the optimized transport model $\chi_i^{\text{opt}} = A_1 \mathcal{L}^x / (A_2 + \tau_{ZF} / \mathcal{L}^{1/2})$ with $\mathcal{L} = a[R/L_{T_i} - \beta R/L_{T_i}^c]$, which is expected to be suitable for the target plasma. Utilizing the optimized model, the transport prediction is performed. However, note that the obtained optimized model will be designed for the target plasma, it will be not universal to general targets. If the plasma condition changes, we have to repeat the same procedures from the step (i) with reconstructed reduced model.

Figure 2 shows the results of the optimized model obtained by the developed scheme for the temperature gradient dependences of the ion heat diffusivity in the case of the ITG turbulent transport in the high- T_i LHD plasma.^{20,21} In this case, we apply the developed scheme to the ion heat transport at radial positions, $\rho = 0.46, 0.50, 0.57, 0.65, 0.72$ and 0.83 in the plasma. Comparing the results of the optimized transport model with the initial transport model, the optimized transport model with the tuned parameters of $\alpha/\alpha_0 = 0.89$ and $\beta/\beta_0 = 0.92$ quite agree with the reference first-principle nonlinear gyrokinetic runs, which are never used for the construction of the optimized model. Indeed, it is confirmed that relative errors among whole

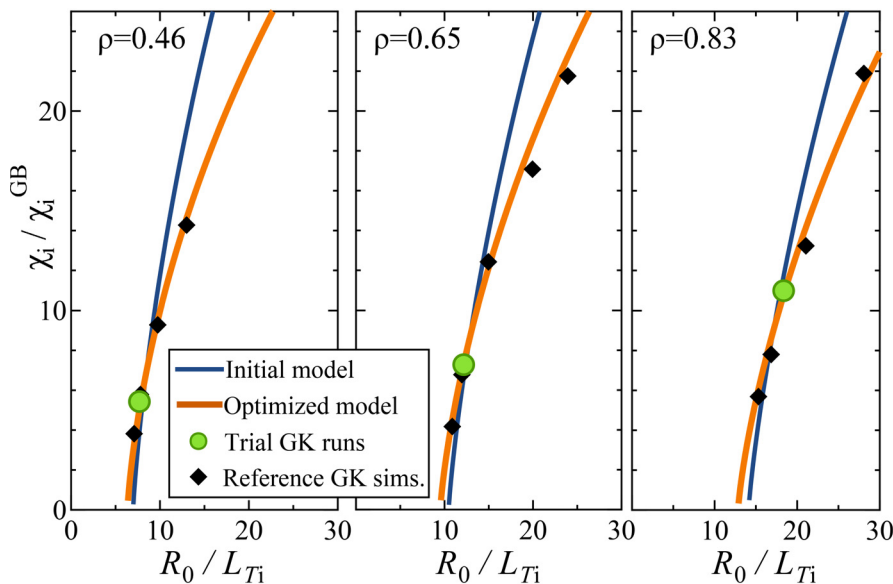


FIG. 2. The temperature gradient dependences of the ion heat diffusivity obtained from the initial model (thin blue curves) and the optimized model (bold orange curves) at $\rho = 0.46, 0.65,$ and 0.83 in the high- T_i LHD plasma. The green circles represent the results of the trial runs for each radial position, and the black diamonds are the reference gyrokinetic simulation results for the reference.

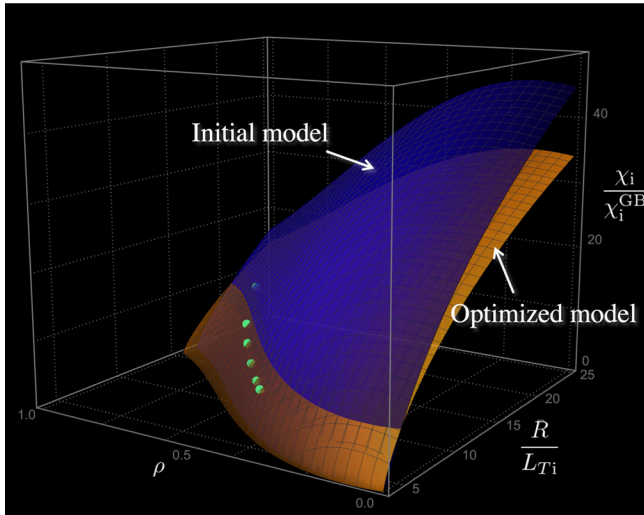


FIG. 3. The result of the optimized transport model χ_i^{opt} in the space of $\{\rho, R/L_{Ti}, \chi_i/\chi_i^{\text{GB}}\}$. For the initial model (blue surface), the trial first-principle simulation at each radial position (green points) is performed and the optimized model (orange surface) is obtained.

radial positions against the results of the reference nonlinear gyrokinetic runs χ_i^{ref} , defined by the root of mean square $\sigma_{\text{model/opt}} \equiv [(1/N_{\text{ref}})\sum_k^{N_{\text{ref}}}(\chi_{i,k}^{\text{model/opt}}/\chi_{i,k}^{\text{ref}} - 1)^2]^{1/2}$, are $\sigma_{\text{opt}} = 0.095$ for the optimized transport model, which is smaller than that of the initial transport model $\sigma_{\text{model}} = 0.35$. Here, N_{ref} is number of the data for the reference simulations. In addition, we confirm that the optimized transport model can reproduce the weakening phenomena of profile stiffness, due to nonlinear effects for higher temperature gradient regions. In Fig. 3, we also plot the whole radial structure of the optimized model while changing the ion temperature gradient.

Furthermore, as shown in Fig. 4, the convergence test of the developed scheme for the tuning parameters, α and β , and the resultant heat diffusivity are performed. In the test, after the step (iii) of the scheme, we return to the step (i) and apply the optimized model χ_i^{opt} instead of the initial model χ_i^{model} , and perform trial gyrokinetic simulations, iteratively. From the figure, it is found that the first execution of the scheme with one trial run of the first-principle nonlinear gyrokinetic simulations for each radial position is enough to construct an optimized transport model. Because of the validity of the initial reduced model Eq. (1), the initial guess of the temperature gradient in the first step (i) can be not so far from the guess by the reference nonlinear gyrokinetic runs. Therefore, required number of the iterations depends on the initial reduced model. At least in this case, the developed scheme can reduce the numbers of first-principle nonlinear gyrokinetic simulation runs to only once for each radial position. Especially in a multi-species case, the reduction efficiency of the scheme for the computation time may be remarkable, because the increase in the numbers of the species expands the multi-dimensional space of the input variables for the first-principle gyrokinetic simulation. Of course, if the number of the parameters in the objective function Eq. (3) increases, we have to increase the number of the radial positions where the trial simulation should be done and find the global

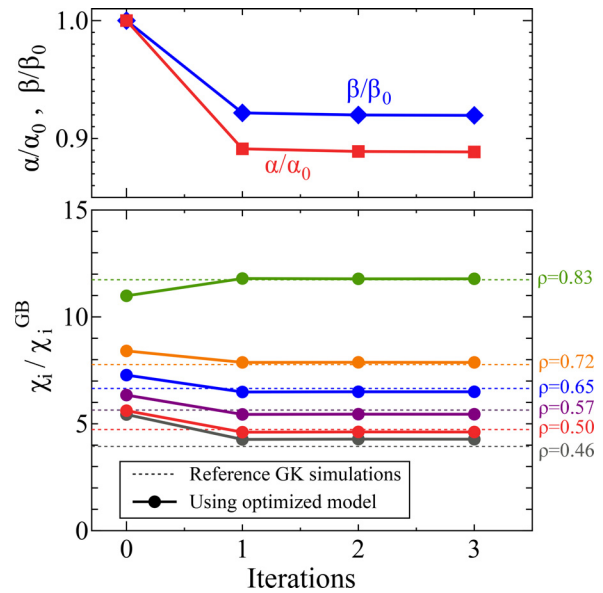


FIG. 4. The convergence test of the iterations of the developed scheme. The top figure represents the convergences of the tuning parameters, α and β , and the bottom figure represents the convergences of the resultant ion heat diffusivity for the radial positions, $\rho = 0.46, 0.50, 0.57, 0.65, 0.72, \text{ and } 0.83$. The dotted lines in the bottom figure represent the results from the reference gyrokinetic simulations.

minimum of the objective function $\sigma(\alpha, \beta, \dots)$ in broader parameter space of $\{\alpha, \beta, \dots\}$. In that case, the calculation cost of the optimization is increased.

C. Radial profiles for transport coefficient and temperature gradient

Using the optimized model, we can obtain the guesses for the ion temperature gradient and the resultant ion heat diffusivity χ_i by performing the nonlinear gyrokinetic simulations at the guessed ion temperature gradients from each transport model, as shown in Fig. 5. Although the temperature gradients guessed by the initial and the optimized transport models are not so different from each other, the results of the diffusivity at the temperature gradients guessed by the optimized model can reproduce the diffusivity at the temperature gradients guessed by the reference simulation better than the initial reduced model. Because of the profile stiffness of the turbulent transport, the slight differences in the temperature gradients lead to clear differences in the heat diffusivity. At least in this application, we can obtain transport levels which quantitatively agree with many nonlinear gyrokinetic simulation results, by using the developed scheme performing one run of the first-principle simulation for each radial position. On the other hand, in the case of the gyrokinetic simulations with kinetic electrons, the guess about the temperature gradient changes, as discussed in our previous work.²² Nevertheless, the developed scheme can be useful in that case, because the scheme is designed to reproduce the reference nonlinear gyrokinetic simulation results in each case of the employed simulations and the corresponding reduced models. Since the developed scheme enables us to thoroughly reduce the numbers of first-principle simulations to obtain the turbulent

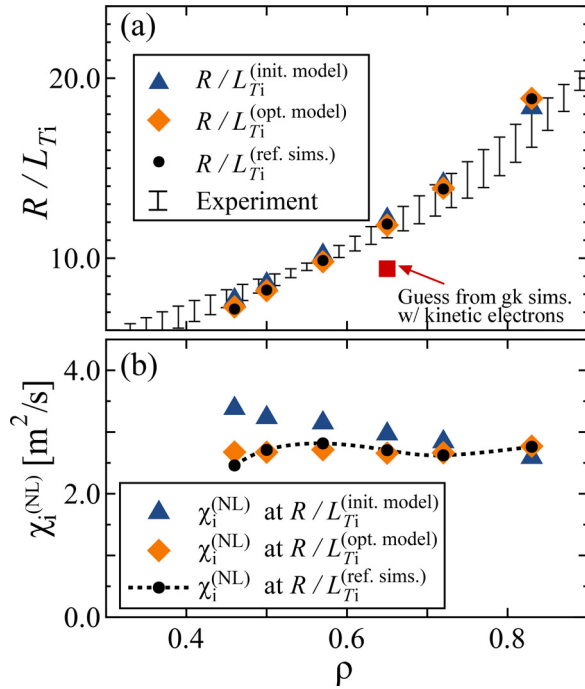


FIG. 5. Radial profiles of (a) the guesses of the ion temperature gradients $R/L_{T_i}^{(\text{guess})}$ using the initial model (blue triangles) denoted by $R/L_{T_i}^{(\text{init. model})}$, the optimized model (orange diamonds) $R/L_{T_i}^{(\text{opt. model})}$, and the reference gyrokinetic simulation results (black circles) $R/L_{T_i}^{(\text{ref. sims.})}$. The error bars represent the experimental results. Radial profile of (b) the nonlinear gyrokinetic simulation results of the ion heat diffusivity $\chi_i^{(NL)}$ at each guessed temperature gradients obtained from the initial model (blue triangles), the optimized model (orange diamonds), and the reference gyrokinetic simulations (black circles) for the high- T_i LHD plasma. In (a), the red square at $\rho = 0.65$ represents the guess from the gyrokinetic simulations with the kinetic electrons for the reference.

transport fluxes, the scheme can be applied to the integrated transport code for quick and precise predictions of the plasma profiles under operation scenarios with saved computational resources, as discussed in Sec. II B.

III. APPLICATION TO TRANSPORT ANALYSIS

In this section, we consider the application of the developed scheme to the transport analysis for ion heat in the high- T_i plasma in the LHD, No. 88 343.^{20,21} The dynamics of the radial profile of the ion temperature can be simulated by solving the diffusion equation written in

$$\frac{\partial}{\partial t} \left(\frac{3}{2} n_i T_i \right) = - \frac{1}{V'} \frac{\partial}{\partial \rho} (V' Q_i) + P_{\text{hx}} + P_{\text{hi}}, \quad (4)$$

where V is the plasma volume, and the prime symbol represents the radial derivatives, $V' = dV/d\rho$, P_{hx} is the heat exchange term, P_{hi} is the absorbed power of the ions, and

$$Q_i = - \langle |\nabla \rho|^2 \rangle n_i \left(\chi_i^{\text{neo}} + \chi_i^{\text{turb}} \right) \frac{\partial T_i}{\partial \rho}, \quad (5)$$

includes the neoclassical contribution χ_i^{neo} and the turbulent contribution χ_i^{turb} for the ion heat transport flux. Here, the bracket $\langle \dots \rangle$ denotes the magnetic flux surface average. The ion heat transport flux Q_i does not contain the convective part, because the core particle source can be negligible, compared with the edge region.

For the turbulent contribution χ_i^{turb} , it is impossible to perform the first-principle nonlinear gyrokinetic simulations at each time step in the evolution. Therefore, we employ the optimized transport model χ_i^{opt} obtained in the previous section, instead of χ_i^{turb} in Eq. (5). Regarding the neoclassical contribution, we employ the DGN/LHD database with a low- β limit.²³ The radial electric field E_r is assumed to be determined by an ambipolar condition at the initial plasma state, and there are three roots which satisfy the ambipolar condition for $0.27 \leq \rho \leq 0.80$, as discussed in the reference.¹⁴ Here, we employ the positive root of the ambipolar electric field in the three roots region, and the profile of the electric field is assumed to be dynamically fixed in the transport analysis. Under the above conditions, we solve the diffusion equation Eq. (4) for the ion heat transport.

Figure 6 shows the comparison of results of the stationary radial profiles for the ion heat diffusivity, using the initial reduced model χ_i^{model} , and the optimized transport model χ_i^{opt} . Here, we fix the temperature profile to the initial state for $0.8 \leq \rho \leq 1.0$, and we calculate the radial profile for the absorbed power of ions P_{hi} , using TASK3D code²⁴ at the initial state and it is dynamically fixed. The steep changes of the heat diffusivity around $\rho \sim 0.27$ in Fig. 6 are caused by the changes of signs of the ambipolar radial electric field, due to a bifurcation from the single root region to the three roots region. Since the ion temperature gradients are in a marginal region of the ITG instability, the stationary profile of the heat diffusivity obtained in the analysis with the optimized transport model is larger than the result with the initial reduced model for the whole radial region. Also, the result is different from Fig. 5(b) because the plot in Fig. 6 is the result of the

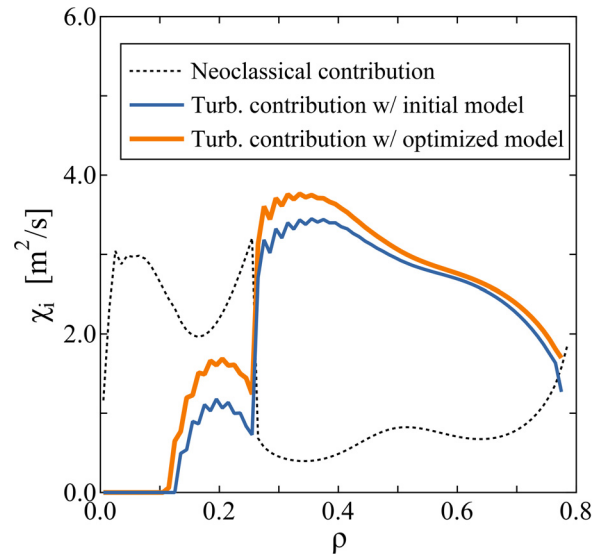


FIG. 6. Stationary radial profiles of ion heat diffusivity obtained from the transport analyses using the initial reduced transport model χ_i^{model} (blue curve) and the optimized transport model χ_i^{opt} (orange curve) for the turbulent contribution. The dotted curve represents the neoclassical contribution χ_i^{neo} obtained from the DGN/LHD database.

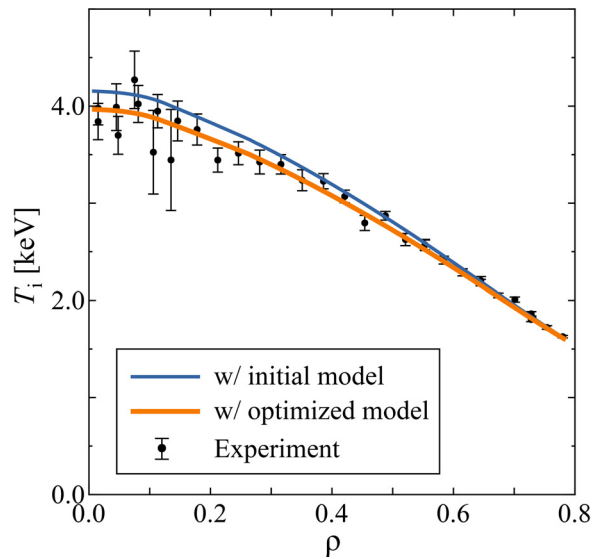


FIG. 7. Radial profiles of the ion temperatures obtained from the transport analyses using the initial reduced transport model χ_i^{model} (blue dashed curve) and the optimized transport model χ_i^{opt} (orange curve) for the turbulent contribution. The error bars represent the experimental observation in the high- T_i LHD plasma.

stationary radial profiles from the transport analysis of the ion temperature profile dynamics. This means that the optimized transport model may contribute to decrease the radial profile of the ion temperature. Indeed, as shown in Fig. 7, we can confirm that the result from the transport analysis with the optimized transport model realizes the moderated radial profile of the ion temperature, compared with the result with the initial reduced model.

For validation against the experimental results, in Fig. 7, we can find there are certain agreement between the results by optimized model and the experimental result for the ion temperature profiles. This reflects that the gyrokinetic simulation with adiabatic electron assumption may reproduce the experimental transport fluxes in the LHD plasmas.²⁵ However, it has been also confirmed that the results of the nonlinear gyrokinetic simulations with kinetic electrons in the LHD plasma is somewhat different from the experimental observations for the temperature gradients as shown in Fig. 5(a). Therefore, we have to perform the validation analyses with further extended transport model including not only the kinetic electron effect but also the other effects such as $E \times B$ shearing. Even if the first-principle nonlinear gyrokinetic simulation does not agree with the experimental observations, however, the developed scheme can estimate the turbulent transport fluxes at least within given physical model based on the gyrokinetic simulations, because the scheme is developed to reproduce the first-principle gyrokinetic simulation results within the simulation conditions. Therefore, the proposed scheme may be helpful to quantitatively estimate the discrepancies between the gyrokinetic simulation and the experiment in order to clarify the validity of the physical model employed in the simulation.

IV. SUMMARY

While the present local gyrokinetic simulations become a reliable way to predict the turbulent transport or the profiles of plasma

temperatures and densities as a first-principle calculation, the quantitative predictions of the transport fluxes strongly demand numerous gyrokinetic runs, in terms of the flux-matching technique against the experimental observations. In this work, by combining the first-principle gyrokinetic simulations, the reduced transport model, and the mathematical optimization techniques, we develop the new scheme to reproduce the first-principle simulation results for the transport prediction, reducing the numbers of nonlinear gyrokinetic simulation runs as much as possible, keeping the accuracy of estimates of the turbulent transport levels. The developed scheme enables us to obtain the optimized transport model for the target plasma by a few run of the nonlinear gyrokinetic simulation at each radial position. It is confirmed that the optimized transport model can achieve reliable and efficient accuracy for the estimate of the turbulent ion heat diffusivity and the ion temperature gradient profile, without the least difference from many runs of the first-principle gyrokinetic simulations.

In the application of the optimized transport model to the transport analysis for the ion heat in the LHD plasma, we confirmed that the stationary profile of the heat diffusivity from the transport analysis with the optimized transport model is slightly larger than the results with the initial reduced model for the marginal temperature gradients. The resultant ion temperature profiles are moderated, compared with the initial reduced model, due to the enhanced heat diffusivity in the optimized model.

Although the calculations and the application of the developed scheme elaborated in this paper are limited to the simple example of ion heat transport driven by the ITG turbulence, with certain tuned common parameters of the transport model, the scheme could be extended to broader case such as a multi-species system. In such a case, we should consider multiple input variables consists of radial gradients of the temperatures and densities for each species and more common parameters. Before the application of the scheme, of course, we have to prepare a reduced model function using each variable as other issues. We should also perform the optimization of the objective function with in broader parameter space $\{\alpha, \beta, \dots\}$. Since the optimized model is designed for the target plasma, if the plasma condition changes, the same procedures should be repeated. Furthermore, to find the relevant guess parameters for trial runs of first-principle simulations, we may have to consider a kind of multi-objective optimization.²⁶ However, even if there is no exact solution to the multi-objective problem, mathematical optimization techniques may be applied to find the maximum likelihood of a solution to the problem. The application of the developed scheme to the case of multi-objective optimization also still remains as future work.

ACKNOWLEDGMENTS

The authors would like to thank the LHD experiment group. This work was supported in part by the Japanese Ministry of Education, Culture, Sports, Science and Technology, Grant (Nos. 19H01879, 19K03801, 20K03907, 21K03514, and 21H04458), by National Institute for Fusion Science (NIFS) collaborative Research Program (Nos. NIFS19KN'TT050, NIFS20KNST161, NIFS21KNST071, NIFS22KIPT005, NIFS22KIPT004, and NIFS22KIST013), by the Collaborative Research Program of Research Institute for Applied Mechanics, Kyushu University (Nos. 2020FP-1, 2021FP-14, and 2022S2-CD-2), by the FLAGSHIP2020,

MEXT within the priority study 6, and by MEXT as the “Program for Promoting Research studies on the Supercomputer Fugaku” (Exploration of burning plasma confinement physics, No. JPMXP1020200103). The numerical results were obtained by using the K computer at the RIKEN Advanced Institute for Computational Science (Proposal number hp180083), JFRS-1 system at International Fusion Energy Research Center (Project Code: GDKTHEL), the supercomputer “Flow” at Information Technology Center, Nagoya University, and “Plasma Simulator” at NIFS.

AUTHOR DECLARATIONS

Conflict of Interest

The authors have no conflicts to disclose.

Author Contributions

Masanori Nunami: Conceptualization (lead); Formal analysis (lead); Funding acquisition (lead); Investigation (lead); Methodology (lead); Visualization (lead); Writing – original draft (lead); Writing – review & editing (lead). **Shinichiro Toda:** Conceptualization (supporting); Data curation (supporting); Formal analysis (supporting); Investigation (supporting). **Motoki Nakata:** Conceptualization (supporting). **Hideo Sugama:** Conceptualization (supporting); Writing – review & editing (supporting).

DATA AVAILABILITY

The data that support the findings of this study are available from the corresponding author upon reasonable request.

REFERENCES

- X. Garbet, Y. Idomura, L. Villard, and T. H. Watanabe, *Nucl. Fusion* **50**, 043002 (2010).
- M. Nakata, M. Honda, M. Yoshida, H. Urano, M. Nunami, S. Maeyama, T.-H. Watanabe, and H. Sugama, *Nucl. Fusion* **56**, 086010 (2016).
- M. Nunami, M. Nakata, S. Toda, A. Ishizawa, R. Kanno, and H. Sugama, *Phys. Plasmas* **25**, 082504 (2018).
- M. Nunami, M. Nakata, S. Toda, and H. Sugama, *Phys. Plasmas* **27**, 052501 (2020).
- F. Warmer, K. Tanaka, P. Xanthopoulos, M. Nunami, M. Nakata, C. D. Beidler, S. A. Bozhenkov, M. N. A. Beurskens, K. J. Brunner, O. P. Ford *et al.*, *Phys. Rev. Lett.* **127**, 225001 (2021).
- J. Candy, C. Holland, R. E. Waltz, M. R. Fahey, and E. Belli, *Phys. Plasmas* **16**, 060704 (2009).
- T. Görler, A. E. White, D. Told, F. Jenko, C. Holland, and T. L. Rhodes, *Phys. Plasmas* **21**, 122307 (2014).
- J. Weiland, *Collective Modes in Inhomogeneous Plasmas and Advanced Fluid Theory*, IOP Series in Plasma Physics (Taylor and Francis, London, 2000).
- G. M. Stabler, J. E. Kinsey, and R. E. Waltz, *Phys. Plasmas* **14**, 055909 (2007).
- J. Citrin, C. Bourdelle, P. Cottier, D. F. Escande, Ö. D. Gürçan, D. R. Hatch, G. M. D. Hogewij, F. Jenko, and M. J. Pueschel, *Phys. Plasmas* **19**, 062305 (2012).
- M. Nunami, T.-H. Watanabe, and H. Sugama, *Phys. Plasmas* **20**, 092307 (2013).
- Y. Takeiri, T. Morisaki, M. Osakabe, M. Yokoyama, S. Sakakibara, H. Takahashi, Y. Nakamura, T. Oishi, G. Motojima, S. Murakami *et al.*, *Nucl. Fusion* **57**, 102023 (2017).
- T.-H. Watanabe and H. Sugama, *Nucl. Fusion* **46**, 24 (2006).
- S. Toda, M. Nunami, A. Ishizawa, T.-H. Watanabe, and H. Sugama, *J. Phys.: Conf. Ser.* **561**, 012020 (2014).
- M. Abadi, A. Agarwal, P. Barham, E. Brevdo, Z. Chen, C. Citro, G. S. Corrado, A. Davis, J. Dean, M. Devin *et al.*, “TensorFlow: Large-scale machine learning on heterogeneous distributed systems,” *arXiv:1603.04467* (2016).
- S. Ruder, “An overview of gradient descent optimization algorithms,” *arXiv:1609.04747* (2016).
- D. P. Kingma and J. Ba, “ADAM: A method for stochastic optimization,” *arXiv:1412.6980* (2014).
- K. Levenberg, *Quart. Appl. Math.* **2**, 164 (1944).
- D. W. Marquardt, *J. Soc. Ind. Appl. Math.* **11**, 431 (1963).
- K. Ida, M. Yoshinuma, M. Osakabe, K. Nagaoka, M. Yokoyama, H. Funaba, C. Suzuki, T. Ido, A. Shimizu, I. Murakami, N. Tamura, H. Kasahara, Y. Takeiri, K. Ikeda, K. Tsumori, O. Kaneko, S. Morita, M. Goto, K. Tanaka, K. Narihara, T. Minami, I. Yamada, and LHD Experimental Group, *Phys. Plasmas* **16**, 056111 (2009).
- K. Tanaka, C. Michael, L. Vyacheslavov, H. Funaba, M. Yokoyama, K. Ida, M. Yoshinuma, K. Nagaoka, S. Murakami, A. Wakasa *et al.*, *Plasma Fusion Res.* **5**, S2053 (2010).
- A. Ishizawa, T.-H. Watanabe, H. Sugama, M. Nunami, K. Tanaka, S. Maeyama, and N. Nakajima, *Nucl. Fusion* **55**, 043024 (2015).
- A. Wakasa, S. Murakami, M. Itagaki, and S. Oikawa, *Jpn. J. Appl. Phys.* **46**, 1157 (2007).
- M. Yokoyama, A. Wakasa, R. Seki, M. Sato, S. Murakami, C. Suzuki, Y. Nakamura, A. Fukuyama, and LHD Experiment Group, *Plasma Fusion Res.* **7**, 2403011 (2012).
- M. Nunami, T.-H. Watanabe, H. Sugama, and K. Tanaka, *Phys. Plasmas* **19**, 042504 (2012).
- K. Deb, “Multi-Objective optimization,” *Search Methodologies* (Springer US, 2014), p. 403.